Materials Physics and Mechanics 47 (2021) 697-705
Research article
Received: October 17, 2021
Accepted: October 18, 2021

MULTI-STEP DILATATIONAL INCLUSION IN AN ELASTICALLY ISOTROPIC CYLINDER

A.L. Kolesnikova[1,2]✉, A.E. Romanov[2,3], M.Yu. Gutkin[1,2,4], V.E. Bougrov[2]

[1]Institute for Problems in Mechanical Engineering, Russian Academy of Sciences, 61 Bolshoj pr., V.O., St. Petersburg, 199178, Russia

[2]ITMO University, 49 Kronverksky pr., St. Petersburg, 197101, Russia

[3]Ioffe Physical-Technical Institute RAS, 26 Polytechnicheskaya, St. Petersburg, 194021, Russia

[4]Highest School of Mechanics and Control Processes, Peter the Great St. Petersburg Polytechnic University, 29 Polytechnicheskaya, St. Petersburg, 195251, Russia

✉ anna.kolesnikova.physics@gmail.com

Abstract. We consider an elastic inclusion in a cylinder with isotropic materials properties. The inclusion possesses a multi-step dependence of the dilatational eigenstrain along the cylinder axis. Basing on the solution for the trace of the stress tensor of the dilatational inclusion with sharp boundaries (single-step inclusion) the stored elastic energy of the multi-step inclusion is determined and analyzed. Then, the found analytical solution for the inclusion energy is used to investigate the energy properties of the transition region between the cylinder domains with a constant level of dilatational eigenstrain. The application of the obtained results to the relevant physical problems of mechanical behavior of hybrid nanodisk/nanowire (ND/NW) semiconductor heterostructures is discussed.

Keywords: dilatational inclusion (DI), eigenstrain, elastic cylinder, elastic strain energy, nanodisk/nanowire hybrid structure

Acknowledgment. *This work was supported by the Ministry of Science and Higher Education of the Russian Federation, research project no. 2019-1442.*

Citation: Kolesnikova A.L., Romanov A.E., Gutkin M.Yu., Bougrov V.E. Multi-step dilatational inclusion in an elastically isotropic cylinder // Materials Physics and Mechanics. 2021, V. 47. N. 5. P. 697-705. DOI: 10.18149/MPM.4752021_4.

1. Introduction

Many practical applications use elastic cylinders as an important element: these can be loaded macro-objects in building construction [1], centimeter size working parts of various machines [2], or broadly used components in modern nanowire (NW) electronics and optoelectronics [3,4]. Elastic response of such objects with cylinder geometry on mechanical or thermal loading is the subject of numerous original works, see e.g., Refs. [5-8], monographs, and textbooks [9-11].

In this study, we focus on the elasticity of a circular cylinder that possesses a prescribed *eigenstrain,* the well-known examples of which are thermal expansion, deformation associated with phase transformation, crystal lattice mismatch, and plastic deformation. When eigenstrain is nonuniform in the cylinder interior, stresses and stored elastic strain energy

http://dx.doi.org/10.18149/MPM.4752021_4

appear in an otherwise mechanically unloaded cylinder. In principle, the eigenstrain can be nonuniform in axial, radial, or azimuthal directions. Due to the characteristic geometry of the cylinder, the axial variation in the eigenstrain plays the most prominent role. When the eigenstrain is localized in a finite domain of the cylinder one can also consider such a configuration as an elastic Eshelby-like inclusion [12].

At present, analytical solutions for a number of elasticity problems for cylinders with axially nonuniform eigenstrain have been reported. The solution for the elastically isotropic cylinder with a single finite size axial region (inclusion) with sharp boundaries and with dilatational eigenstrain was given in Ref. [13]. The found in this work result was used to determine elastic properties for the infinite row of dilatational inclusions (DIs) in a cylinder [14] and was also expanded to the case of a single DI in a cylinder made of transversally isotropic material [15]. The latter finding was rediscovered in a different form in Ref. [16]. Finally, in our recent works [17,18] the results were given on the elastic properties of DIs for the cases of sharp and blurred (diffused) boundaries with linearly or exponentially varying eigenstrain in the cylinder axial direction.

In this paper, we develop an approach to determine the elastic field and associated elastic energy in an elastically isotropic circular cylinder with DI demonstrating step-like dependence of the dilatational eigenstrain along the cylinder axis. Such multi-step DIs can be useful to model strain-stress state in experimentally observed hybrid nanodisk/nanowire (ND/NW) semiconductor heterostructures [19-21].

2. Background: single-step dilatational inclusion

We consider an elastically isotropic circular cylinder (see Fig. 1) of radius a, in which there exists an axially varying dilatational eigenstrain $\varepsilon^*(z)$:

$$\varepsilon^*_{rr} = \varepsilon^*_{\varphi\varphi} = \varepsilon^*_{zz} = \varepsilon^*(z)\,, \tag{1a}$$

$$\varepsilon^*_{xx} = \varepsilon^*_{yy} = \varepsilon^*_{zz} = \varepsilon^*(z)\,, \tag{1b}$$

where either cylindrical r,φ,z, or Cartesian coordinates z,y,z are used, respectively. For practically important cases, function $\varepsilon^*(z)$ can be constant in the domain $z_1 < z < z_2$ separated by the transition regions from the rest of the cylinder volume, where it is assumed to be zero, see Fig. 1.

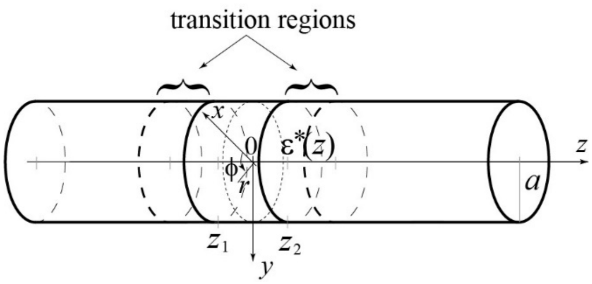

Fig. 1. Schematics of a circular cylinder with axial nonuniform dilatational eigenstrain $\varepsilon^*(z)$ localized in the domain $z_1 < z < z_2$ plus transition regions. Cartesian (x, y, z) and cylindrical (r,φ, z) coordinate systems are shown

In general, the eigenstrain is defined as a stress-free deformation with respect to a reference state [22]. From a physical point of view eigenstrain can be described as a change in the lattice constant of the material (for simplicity we deal with cubic materials with a single lattice constant) from the initial value a_i to a final value a_f :

$$\varepsilon^* = \frac{a_f - a_i}{a_i}. \quad (2)$$

For a finite domain with different chemical composition (and hence with unequal lattice constants) observed in NWs, it is natural to define eigenstrain as a lattice mismatch ε_m that is peculiar to the heterointerfaces, which bound the domain under consideration. These heterointerfaces (boundaries) can be either sharp (abrupt or localized) [19, 23] or smooth (diffuse or blurred) [24,25] in the direction of NW axis. One can also analyze a single heterointerface (or transition regions) separating two parts of a NW of infinite extend [17,18,26,27].

In Ref. [17], the technique was proposed for finding the elastic fields in an isotropic cylinder with a prescribed distribution of the eigenstrain $\varepsilon^*(z)$ by utilizing the solution for infinitesimally thin dilatational disk in the form of convolution with weight function $\varepsilon^*(z)$. Then, in Ref. [18], the solutions for elastic fields and stored strain energy for individual DIs with sharp and blurred boundaries were given in full detail.

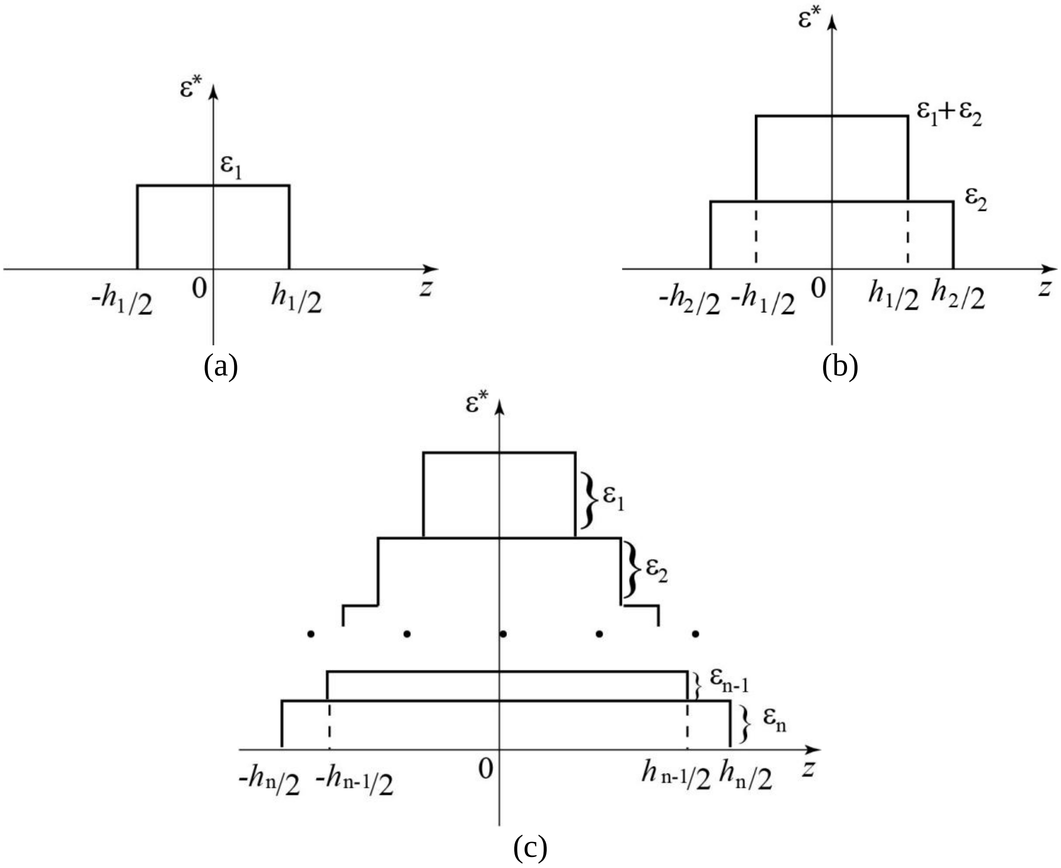

Fig. 2. Distributions of eigenstrain $\varepsilon^*(z)$ in a cylinder with dilatational inclusions (DIs) were used for modeling hybrid ND/NW heterostructures.
(a) $\varepsilon^*(z)$ for single-step DI – sDI; (b) $\varepsilon^*(z)$ for double-step DI – dDI;
(c) $\varepsilon^*(z)$ for multi-step DI – nDI

The eigenstrain function shown in Fig. 2a is written as

$$\varepsilon^*(z) = \varepsilon_1 H\left[\frac{h_1}{2} - |z|\right] H\left[r - a\right], \qquad (3)$$

where ε_1 is the magnitude of the eigenstrain, $H[p]$ is the Heaviside step-function, h_1 is the length of the domain with constant eigenstrain, was used in Refs. [17,18] to model hybrid ND/NW heterostructures with well localized boundaries. In the following, we designated this case as a single-step dilatational inclusion (sDI).

All stress tensor components for the sDI can be found in the closed analytical form [18]. Here we only give the formula for the trace ${}^{\rm sDI}\sigma_{ii}$ of stress tensor as a function of coordinates, inclusion length, and magnitude of the eigenstrain:

$$ {}^{\rm sDI}\sigma_{ii}\left(r,z\right) = -\frac{4G(1+\nu)\varepsilon_1}{(1\text{-}\nu)} H\left[\frac{\tilde{h}_1}{2} - |\tilde{z}|\right] H\left[1\text{-}\,\tilde{r}\right] + $$
$$ + \frac{8G(1+\nu)^2\varepsilon_1}{\pi(1-\nu)} \int_0^\infty \frac{I_1 I_0(\tilde{r}\beta)}{\beta^2 I_0^2 - (\beta^2 - 2\nu + 2) I_1^2} \sin\left(\frac{\tilde{h}_1\beta}{2}\right) \cos\tilde{z}\beta \; d\beta \,, \qquad (4)$$

where G and ν are a shear modulus and Poisson ratio of the material of the cylinder, respectively; $I_n(\zeta), n = 0{,}1$ are the modified Bessel functions of the first kind, and for brevity, the notations $I_n = I_n(\beta)$, are introduced. Variables r, z and parameter h_1 are normalized to the radius of the cylinder a: $\tilde{r} = r/a$, $\tilde{z} = z/a$, $\tilde{h}_1 = h_1/a$. One can recognize that the first term in Eq. (4) comes from the stresses of the cylindrical DI in an infinite isotropic medium, whereas the second term arises due to boundary conditions that should be met on the cylinder lateral free surface.

The strain energy of the sDI was determined from the expression given in Ref. [17]:

$$E_{\rm sDI} = -\frac{1}{2}\int_V \varepsilon_{ij}^* \sigma_{ij} dV = -\frac{1}{2}\int_{V_{\rm sDI}} \varepsilon^*(z)\, {}^{\rm sDI}\sigma_{ii}(r,z)\, dV \,, \qquad (5)$$

where the first equality is just the well-known relation [22] for finding the energy associated with an elastic field (stresses σ_{ij}) caused by an eigenstrain ε_{ij}^* in a body with volume V and the second equality provides the result of the application of this relation to the sDI with the volume $V_{\rm sDI}$ placed in the elastic cylinder. As a result, the energy of an isolated sDI was found in the following form [18]:

$$E_{\rm sDI} = \frac{2G(1+\nu)\varepsilon_1^2\pi a^3}{(1\text{-}\nu)} \left\{ \tilde{h}_1 - \frac{8(1+\nu)}{\pi} \int_0^\infty \frac{I_1^{\,2}}{\beta^2[\beta^2 I_0^{\,2} - (\beta^2 - 2\nu + 2) I_1^{\,2}]} \left(\sin\frac{\tilde{h}_1\beta}{2}\right)^2 d\beta \right\}. \qquad (6)$$

In this formula, the first term in the parentheses, i.e., $\tilde{h}_1$, when used with the in front multiplier, defines the energy of cylindrical sDI in an infinite isotropic elastic medium; the second term is responsible for the energy decrease of such sDI due to the screening effect of the lateral cylinder surface.

3. Strain energy of multi-step dilatational inclusion

Double-step DI with eigenstrain dependence shown in Fig. 2b can be constructed as a superposition of two overlapping sDIs with lengths h_1, h_2 and eigenstrain magnitudes $\varepsilon_1, \varepsilon_2$, correspondingly. In such a configuration, the stored in the cylinder elastic strain energy $E_{\rm dDI}$ in addition to self-energies $E_{\rm sDI}^{(1)}$ and $E_{\rm sDI}^{(2)}$ includes interaction energy W:

$$E_{\rm dDI} = E_{\rm sDI}^{(1)}(\varepsilon_1, h_1) + E_{\rm sDI}^{(2)}(\varepsilon_2, h_2) + W(\varepsilon_1, \varepsilon_2, h_1, h_2)\,, \qquad (7)$$

where the dependence of each of energy contributions on the geometrical characteristics of sDIs in the cylinder, is specified, and the interaction energy term can be found from the formula similar to Eq. (5):

$$W(\varepsilon_1, \varepsilon_2, h_1, h_2) = -\varepsilon_2 \int_{V_{\mathrm{sDI2}}} {}^{\mathrm{sDI}}\sigma_{ii}^{(1)}\, dV = \frac{4G(1+\nu)\varepsilon_1 \varepsilon_2 \pi a^3}{(1-\nu)} \tilde{h}_1 -$$
$$-\frac{32G(1+\nu)^2 \varepsilon_1 \varepsilon_2 a^3}{(1-\nu)} \int_0^\infty \frac{I_1^2}{\beta^2[\beta^2 I_0^2 - (\beta^2 - 2\nu + 2) I_1^2]} \sin\frac{\tilde{h}_1\beta}{2} \sin\frac{\tilde{h}_2\beta}{2}\, d\beta, \tag{8}$$

where the trace of the stress tensor is attributed to the first sDI, but the eigenstrain magnitude and the volume are attributed to the second sDI and, as before the normalized values $\tilde{h}_{1,2} = h_{1,2}/a$ are used.

Combining the results given by Eqs. (6) and (8) we get:

$$E_{\mathrm{dDI}} = 2C\varepsilon_1^2\pi \left\{ \tilde{h}_1 - \frac{8(1+\nu)}{\pi} \int_0^\infty A(\beta) \left(\sin\frac{\tilde{h}_1\beta}{2} \right)^2 d\beta \right\} +$$
$$+2C\varepsilon_2^2\pi \left\{ \tilde{h}_2 - \frac{8(1+\nu)}{\pi} \int_0^\infty A(\beta) \left(\sin\frac{\tilde{h}_2\beta}{2} \right)^2 d\beta \right\} +$$
$$+4C\varepsilon_1 \varepsilon_2 \pi \tilde{h}_1 - 32C(1+\nu)\varepsilon_1 \varepsilon_2 \int_0^\infty A(\beta) \sin\frac{\tilde{h}_1\beta}{2} \sin\frac{\tilde{h}_2\beta}{2}\, d\beta. \tag{9}$$

Here, the designations $C = \dfrac{G(1+\nu)a^3}{(1\text{-}\nu)}$ and $A(\beta) = \dfrac{I_1^2}{\beta^2[\beta^2 I_0^2 - (\beta^2 - 2\nu + 2) I_1^2]}$ are introduced.

The found formula for double-step dilatational inclusion energy E_{dDI} can be rearranged by exploring the known integral representations [28]:

$$\frac{\pi}{2} a = \int_0^\infty \frac{1}{\beta^2} (\sin a\beta)^2\, d\beta, \quad \frac{\pi}{2} \min(a,b) = \int_0^\infty \frac{1}{\beta^2} \sin a\beta \sin b\beta\, d\beta \tag{10a,b}$$

and accounted for $h_2 \geq h_1$ to the following form:

$$E_{\mathrm{dDI}} = 8C\varepsilon_1^2 \int_0^\infty B(\beta) \left(\sin\frac{\tilde{h}_1\beta}{2} \right)^2 d\beta + 8C\varepsilon_2^2 \int_0^\infty B(\beta) \left(\sin\frac{\tilde{h}_2\beta}{2} \right)^2 d\beta +$$
$$+16C\varepsilon_1 \varepsilon_2 \int_0^\infty B(\beta) \sin\frac{\tilde{h}_1\beta}{2} \sin\frac{\tilde{h}_2\beta}{2}\, d\beta, \tag{11}$$

where $B(\beta) = \dfrac{\beta^2 I_0^2 - \beta^2 I_1^2 - 4I_1^2}{\beta^2[\beta^2 I_0^2 - (\beta^2 - 2\nu + 2) I_1^2]}$.

Finally, the similarity of integrals in Eq. (11) makes it possible to rewrite the formula for the energy of double-step dilatational inclusion in an elastically isotropic cylinder in the following compact form:

$$E_{\mathrm{dDI}} = 8C \sum_{i,j=1}^{2} \varepsilon_i \varepsilon_j \int_0^\infty B(\beta) \sin\frac{\tilde{h}_i\beta}{2} \sin\frac{\tilde{h}_j\beta}{2}\, d\beta. \tag{12}$$

When using such compact notation of the formula, one must count the interaction energy term twice since there is the multiplier "16" but not "8" in Eq. (11).

The found result allows us to find the energy E_{nDI} of multi-step configuration with the eigenstrain showing n steps (see Fig. 2c):

$$E_{\mathrm{nDI}} = 8C\sum_{i,j=1}^{n} \varepsilon_i \varepsilon_j \int_0^\infty B(\beta)\sin\frac{\tilde{h}_i \beta}{2}\sin\frac{\tilde{h}_j \beta}{2} d\beta . \tag{13}$$

If the length h_1 of the central part of the multi-step DI becomes much larger than the cylinder radius a and the lengths of other parts h_k, $k = 2\ldots n$, are related to h_1 via length differences $2\Delta h_k$ of a finite magnitude:

$$h_k = h_1 + 2\Delta h_k , \tag{14}$$

the energy of the system can be considered as the energy of two heterointerfaces (boundaries) with step-like eigenstrain transition regions. As a result, the energy E_{nB} of such multi-step transition region is:

$$E_{\mathrm{nB}} = \frac{1}{2}\lim_{h_{i,j}\to\infty} E_{\mathrm{nDI}} = 4C\sum_{i=1}^{n} \varepsilon_i^2 \lim_{h_i\to\infty}\int_0^\infty B(\beta)\left(\sin\frac{\tilde{h}_i \beta}{2}\right)^2 d\beta +$$

$$+8C\lim_{h_1\to\infty}\sum_{i,j=1}^{n} \varepsilon_i \varepsilon_j \int_0^\infty B(\beta)\sin\frac{(\tilde{h}_1 + 2\Delta\tilde{h}_i)\beta}{2}\sin\frac{(\tilde{h}_1 + 2\Delta\tilde{h}_j)\beta}{2} d\beta =$$

$$=2C\sum_{i=1}^{n}\varepsilon_i^2\int_0^\infty B(\beta)d\beta + 4C\sum_{\substack{i,j=1,\\ i\neq j}}^{n} \varepsilon_i \varepsilon_j \int_0^\infty B(\beta)\cos(\Delta\tilde{h}_i - \Delta\tilde{h}_j)\beta\, d\beta . \tag{15}$$

where, as usual, we use normalized values $\Delta\tilde{h}_k = \Delta h_k / a$. Note that in Eq. (15), we need to calculate the *ij*-interaction energy term once.

For the uniform distribution of eigenstrain steps with $\varepsilon_k = \varepsilon_0 / n$ and $2\Delta h = h_{k+1} - h_k$, $h_k = h_1 + 2(k-1)\Delta h$, $\Delta h_k = (k-1)\Delta h$, $\Delta\tilde{h} = \Delta h / a$ for the energy E_{nB} of the transition region we find:

$$E_{\mathrm{nB}} = \frac{2C\varepsilon_0^2}{n}\int_0^\infty B(\beta)d\beta + \frac{4C\varepsilon_0^2}{n^2}\int_0^\infty B(\beta)\sum_{\substack{i,j=1,\\ i\neq j}}^{n}\cos(i-j)\Delta\tilde{h}\beta\, d\beta = \frac{2C\varepsilon_0^2}{n^2}\int_0^\infty B(\beta)\frac{\cos n\Delta\tilde{h}\beta - 1}{\cos\Delta\tilde{h}\beta - 1} d\beta . \tag{16}$$

4. Discussion and Conclusions

It was found in our earlier work, see Ref. [18], that the dependence of the elastic strain energy of the single-step dilatational inclusion (sDI) on its lateral size h_1 exhibits a maximum at $h_1 \approx 0.6a$ (for Poisson ratio $\nu = 0.3$) with a being cylinder radius. The same property, i.e., the presence of maximum, remains for multi-step DI when its size increases with a fixed structure of steps. The difference, however, appears in the saturation values of the energy at $h_1 \to \infty$. These values characterize the doubled energy of the transition region (step boundary) E_{nB} with the prescribed step structure, see Eq. (15).

One can also analyze the energy of the step boundary E_{nB} (in the case of equal length of the steps) as a function of the step length Δh for a various number of steps *n*. Such dependencies are plotted in Fig. 3 for cases n = 2 and 3. Again, for $\Delta h \to \infty$ the energy saturates to the value of the sum energy of 2 of 3 sharp boundaries with dilatation jump $\varepsilon_0 / 2$ or $\varepsilon_0 / 3$, correspondingly. An interesting feature of the dependencies shown in Fig. 3 is the appearance of shallow minima at $\Delta h < a$. With n increasing the position of the minimum shifts to smaller Δh .

In the other case when $\Delta\tilde{h} = \tilde{\Delta}/(n-1)$ and $n \to \infty$, formula (16) transforms to the following:

$$\lim_{n\to\infty} E_{\mathrm{nB}} = \lim_{n\to\infty} \frac{2C\varepsilon_0^2}{n^2} \int_0^\infty B(\beta) \frac{\cos[n\tilde{\Delta}\beta/(n-1)]-1}{\cos[\tilde{\Delta}\beta/(n-1)]-1} d\beta = \frac{8C\varepsilon_0^2}{\tilde{\Delta}^2} \int_0^\infty B(\beta)\left(\sin\frac{\tilde{\Delta}\beta}{2}\right)^2 d\beta \ . \tag{17}$$

Such a configuration corresponds to the diminishing of the individual dilatation step length with a fixed length of the transition region Δ. The found energy coincides with that one for the boundary with linear blur studied in Ref. [18].

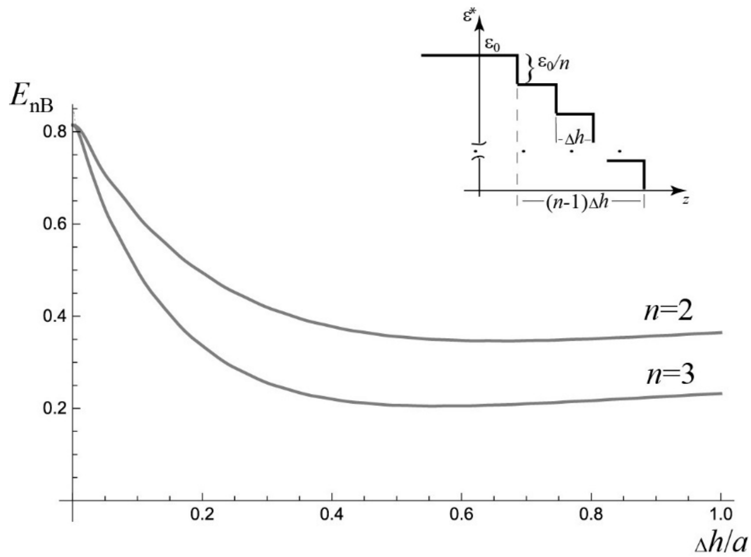

Fig. 3. Energy of the multi-step boundary E_{nB} as a function of the step length Δh for a different number of steps *n* is shown. The energy is given in units $G\varepsilon_0^2 a^3$, where G is the shear modulus, ε_0 is the maximum eigenstrain value, a is the radius of the cylinder. Plots are presented for Poisson ratio $\nu = 0.3$

It has been already mentioned that transition regions with both sharp and smooth variations of crystal lattice parameters are experimentally observed in semiconductor NW heterostructures [19-21,23-25]. We propose to use the developed in the present study approach for modeling multi-step dilatational inclusions in an elastic cylinder for the description of such objects. Any observed dependence of crystal lattice parameter in a NW can be approximated with a step-like function that will allow us to utilize the found analytical expressions for elastic fields and stored strain energy. The next step in the analysis will be the investigation of the stability of NW heterostructures with the prescribed distribution of eigenstrain with respect to the formation of various defects, e.g., misfit dislocations. This is the subject of our ongoing study.

In conclusion, the stored elastic energy of the multi-step dilatation inclusion in an elastic cylinder has been determined and analyzed. The analytical solution for the inclusion energy has been used to investigate the energy properties of the transition region between the cylinder domains with a constant level of dilatational eigenstrain. The application of obtained results to the relevant physical problems of mechanical behavior of hybrid nanodisk/nanowire (ND/NW) semiconductor heterostructures has been briefly discussed.

References

[1] Domone PL. A review of the hardened mechanical properties of self-compacting concrete. *Cement & Concrete Composites*. 2007;29(1): 1-12.
[2] Toribio J, Álvarez N, González B, Matos JC. A critical review of stress intensity factor solutions for surface cracks in round bars subjected to tension loading. *Engineering Failure Analysis*. 2009;16(3): 794-809.
[3] Zhang C, Li XL. III-V nanowire transistors for low-power logic applications: a review and outlook. *IEEE Transactions on Electron Devices*. 2016;63(1): 223-234.
[4] Koblmuller G, Mayer D, Stettner T, Abstreiter G. GaAs-AlGaAs core-shell nanowire lasers on silicon: invited review. *Semiconductor Science and Technology*. 2017;32(5): 053001(1-22).
[5] Barton MV. The circular cylinder with a band of uniform pressure on a finite length of the surface. *Journal of Applied Mechanics*. 1941;8: A97-A104.
[6] Tutuncu N, Winckler SJ. Stresses and deformations in thick-walled cylinders subjected to combined loading and a temperature-gradient. *Journal of Reinforced Plastics and Composites*. 1993;12(2): 198-209.
[7] Kollar LP. 3-dimensional analysis of composite cylinders under axially varying hygrothermal and mechanical loads. *Composite Structures*. 1994;50(4): 525-540.
[8] Liu X, Zhang H, Xia M, Wang B, Zheng Q, Wu K. A closed-form solution for stress analysis of hollow cylinder structure under non-uniform external load and its engineering application. *Journal of Engineering Research*. 2020;8(1): 72-88.
[9] Love AEH. *A Treatise on the Mathematical Theory of Elasticity*. Cambridge: Cambridge University Press; 1959.
[10] Lurie AI. *Spatial Problems of Theory of Elasticity*. Moscow: State Publishing House of Scientific and Technical Literature; 1955. (In Russian)
[11] Timoshenko SP, Goodier NJ. *Theory of elasticity*. New York: McGraw Hill; 1970.
[12] Eshelby JD. The determination of the elastic field of an ellipsoidal inclusion and related problems. *Proceedings of the Royal Society A*. 1957;241(1226): 376-396.
[13] Zhong Z, Sun QP, Tong P. On the elastic axisymmetric deformation of a rod containing a single cylindrical inclusion. *International Journal of Solids and Structures*. 2000;37(41): 5943-5955.
[14] Zhong Z, Sun QP, Yu XB. Elastic solutions of a cylindrical rod containing periodically distributed inclusions with axisymmetric eigenstrains. *Acta Mechanica*. 2003;166(1-4): 169-183.
[15] Zhong Z, Sun QP. Analysis of a transversely isotropic rod containing a single cylindrical inclusion with axisymmetric eigenstrain. *International Journal of Solids and Structures*. 2002;39(23): 5753-5765.
[16] Kaganer VM, Belov AYu. Strain and x-ray diffraction from axial nanowire heterostructures. *Physical Review B*. 2012;85(12): 125402(1-9).
[17] Romanov AE, Kolesnikova AL, Gutkin MYu, Dubrovskii VG. Elasticity of axial nanowire heterostructures with sharp and diffuse interfaces. *Scripta Materialia*. 2020;176(1): 42-46.
[18] Romanov AE, Kolesnikova AL, Gutkin Myu. Elasticity of a cylinder with axially varying dilatational eigenstrain. *International Journal of Solids and Structures*. 2021;213(1): 121-134.

[19] Tchernycheva M, Cirlin GE, Patriarche G, Travers L, Zwiller V, Perinetti U, Harmand J-Ch. Growth and characterization of InP nanowires with InAsP insertions. *Nano Letters*. 2007;7(6): 1500-1504.
[20] Sutter E, Sutter P. Axial heterostructures with phase-controlled metastable segments via post growth reactions of Ge nanowires. *Chemistry of Materials*. 2019;31(19): 8174-8181.
[21] Bolshakov AD, Fedorov VV, Sibirev NV, Fetisova MV, Moiseev EI, Kryzhanovskaya NV, Koval OYu, Ubyivovk EV, Mozharov AM, Cirlin GE, Mukhin IS. Growth and characterization of GaP/GaPAs nanowire heterostructures with controllable composition. *Physica Status Solidi RRL*. 2019;13(11): 1900350(1-7).
[22] Mura T. *Micromechanics of Defects in Solids*. Boston: Martinus Nijhoff; 1987.
[23] Priante G, Glas F, Patriarche G, Pantzas K, Oehler F, Harmand JC. Sharpening the interfaces of axial heterostructures in self-catalyzed AlGaAs nanowires: experiment and theory. *Nano Letters*. 2016;16(3): 1917-1924.
[24] Zannier V, Rossi F, Dubrovskii VG, Ercolani D, Battiato S, Sorba L. Nanoparticle stability in axial InAs−InP nanowire heterostructures with atomically sharp interfaces. *Nano Letters*. 2018;18(1): 167-174.
[25] Beznasyuk DV, Stepanov P, Rouviere JL, Glas F, Verheijen M, Claudon J, Hocevar M. Full characterization and modelling of graded interfaces in high lattice-mismatch axial nanowire heterostructures. *Physical Review Materials*. 2020;4(7); 074607(1-7).
[26] Ertekin E, Greaney PA, Chrzan DC. Equilibrium limits of coherency in strained nanowire heterostructures. *Journal of Applied Physics.* 2005;97(11): 114325(1-10).
[27] Glas F. Critical dimensions for the plastic relaxation of strained axial heterostructures in free-standing nanowires. *Physical Review B.* 2006;74(12): 121302(R)(1-4).
[28] Prudnikov AP, Brychkov YuA, Marichev OI. *Integrals and Series*. Moscow: Nauka; 1981. (In Russian)

THE AUTHORS

Kolesnikova A.L.
e-mail: anna.kolesnikova.physics@gmail.com
ORCID: 0000-0003-4116-4821

Romanov A.E.
e-mail: alexey.romanov@niuitmo.ru
ORCID: 0000-0003-3738-408X

Gutkin M.Yu.
e-mail: m.y.gutkin@gmail.com
ORCID: 0000-0003-0727-6352

Bougrov V.E.
e-mail: vladislav.bougrov@itmo.ru
ORCID: 0000-0002-5380-645X